

# Mutant U1A-RNA binding kinetics with surface plasmon resonance

Daniel Park<sup>#, \*, \*\*</sup>, Cody Geoffroy<sup>#, \*</sup>, Nicole Verity\*, Robert Borgon\*, Hajeung Park\*\*

\*Burnett School of Biomedical Sciences, College of Medicine, University of Central Florida, Orlando, FL 32816

\*\*Herbert Wertheim Scripps Institute for Biomedical Innovation and Technology, University of Florida, Jupiter, FL 33458

[#] denotes first authorship; [\*] and [\*\*] denotes research location

## Abstract

Splicing of RNA is a necessary component in protein synthesis in complex organisms. Much of human DNA contains introns which are sequences that must be spliced out of the pre-mRNA transcript. The small nuclear ribonuclear proteins (snRNPs) are responsible for splicing the immature RNA into a coding RNA. An important protein that is involved with the formation of the spliceosome is the snRNP U1. U1 will come together with other snRNPs to create the spliceosome to coordinate the splicing of introns and allow for RNA maturation.

Our research is focused on a protein subunit of U1 named U1A. A mutated plasmid was transformed into E. coli NEB turbo cells. A pET 17b vector then consisted of a HIS tag for purification. The plasmid with the mutations were transformed into E. coli BL21 DE3 competent cells for protein production, sonication, then U1A was purified with an IMAC column.

This mutational study explores binding efficacy of the U1A to the hairpin. Surface plasmon resonance (SPR) was utilized to quantify the binding kinetics of both biological molecules using a nitrilotriacetic acid (NTA) chip. U1A mutations were made at two locations: tyrosine to alanine at position 13 and glutamine to alanine at position 54.

## Materials & Methods

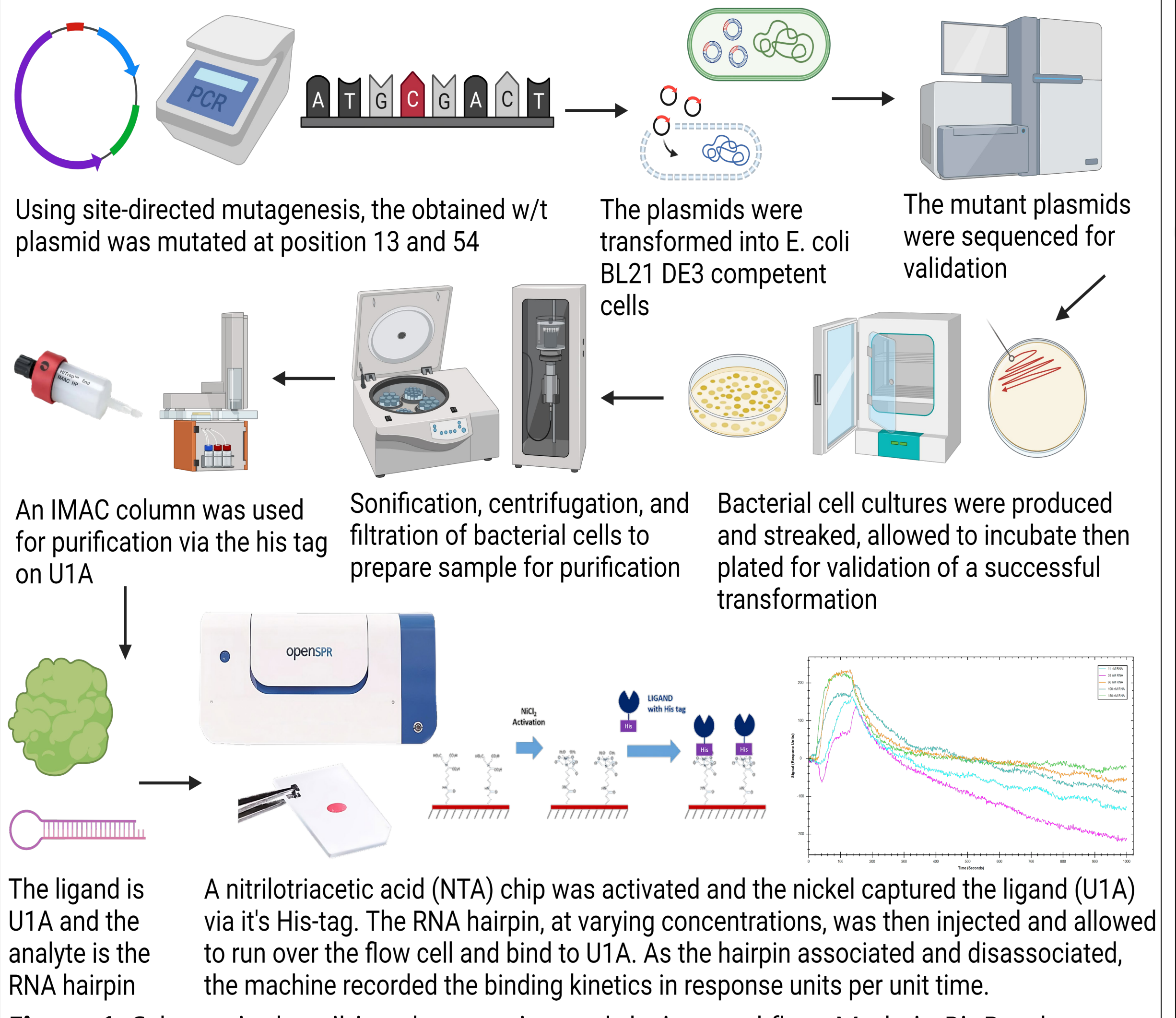


Figure 1: Schematic describing the experimental design workflow. Made in BioRender.

## Results

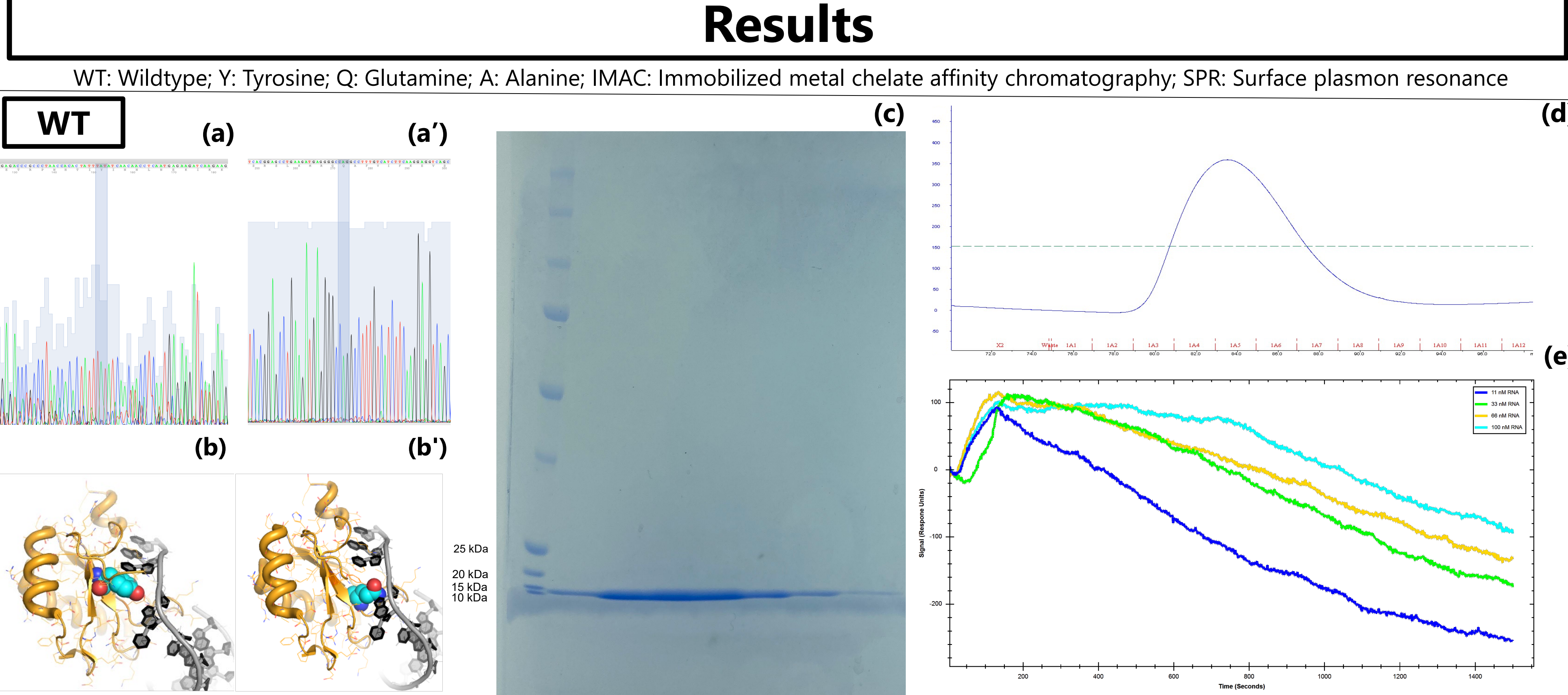


Figure 2: (a) Sequencing spectral data showing region of interest in plasmid containing tyrosine at position 13. (a') Region of interest in plasmid containing glutamine at position 54. (b) U1A wildtype highlighted (cyan) at position 13 (tyrosine). Coordinate from PDB ID 6SQN. (b') U1A wildtype highlighted at position 54 (glutamine). Coordinate from PDB ID 6SQN. (c) SDS-PAGE gel showing expressed w/t U1A domain at approximately 12 kDa. (d) Chromatogram showing absorbance peak of WT U1A following IMAC purification. (e) SPR graph in response units showing association and disassociation curves of the WT (i.e., ligand) to an RNA hairpin (i.e., analyte).

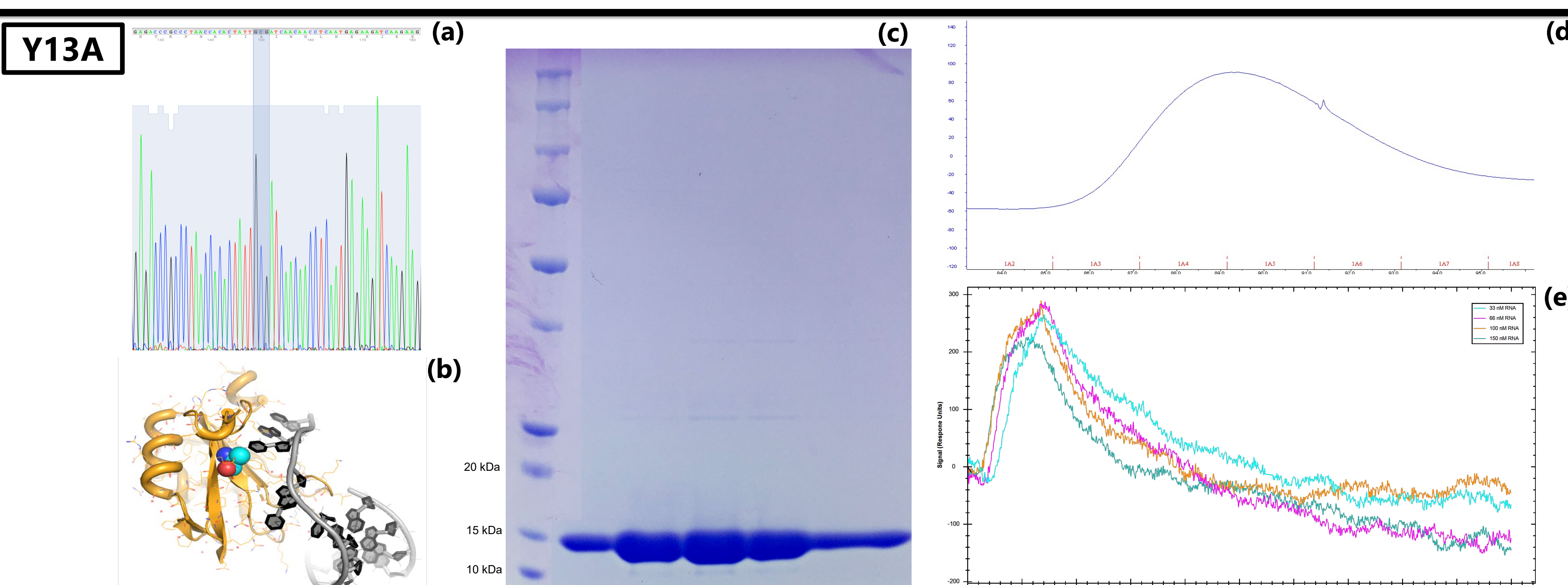


Figure 3: (a) Sequencing spectral data showing region of interest in plasmid containing tyrosine to alanine mutation at position 13. (b) Highlighted (Cyan) is the Y13A mutation. Coordinate from PDB ID 6SQN. (c) SDS-PAGE gel showing expressed mutant Y13A U1A domain at approximately 12 kDa. (d) Chromatogram showing absorbance peak of Y13A mutant following IMAC purification. (e) SPR graph in response units showing association and disassociation curves of the Y13A mutant (i.e., ligand) to an RNA hairpin (i.e., analyte).

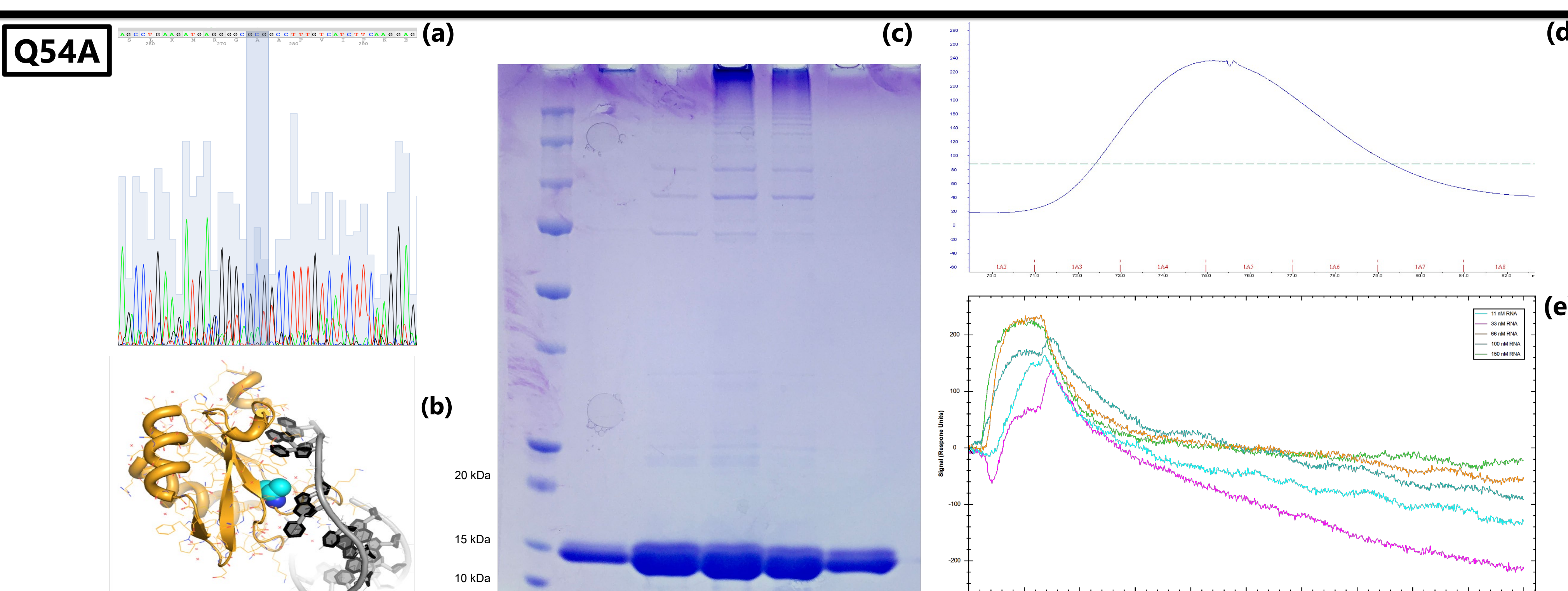


Figure 4: (a) Sequencing spectral data showing region of interest in plasmid containing glutamine to alanine mutation at position 13. (b) Highlighted (cyan) is the Q54A mutation. Coordinate from PDB ID 6SQN. (c) SDS-PAGE gel showing expressed mutant Q54A U1A domain at approximately 12 kDa. (d) Chromatogram showing absorbance peak of Q54A mutant following IMAC purification. (e) SPR graph in response units showing association and disassociation curves of the Q54A mutant (i.e., ligand) to an RNA hairpin (i.e., analyte).

## Results

	$k_a$	$k_d$	$k_D (k_d/k_a)$
WT	1.95E+5	3.67E-3	1.86E-8
Y13A	6.28E+5	1.12E-2	1.78E-8
Q54A	2.50E+5	1.30E-2	5.18E-8

Figure 5: Constant chart for all three major kinetic parameters. A higher  $k_D$  indicates a lower affinity of ligand (U1A) to analyte (RNA hairpin) whereas a lower value indicates a higher affinity. A typical range for  $k_a$ ,  $k_d$ , and  $k_D$  are as follows, respectively:  $10^3$  to  $10^7$ ,  $10^{-1}$  to  $5 \times 10^{-6}$ , and  $10^{-3}$  to  $10^{-2}$ .

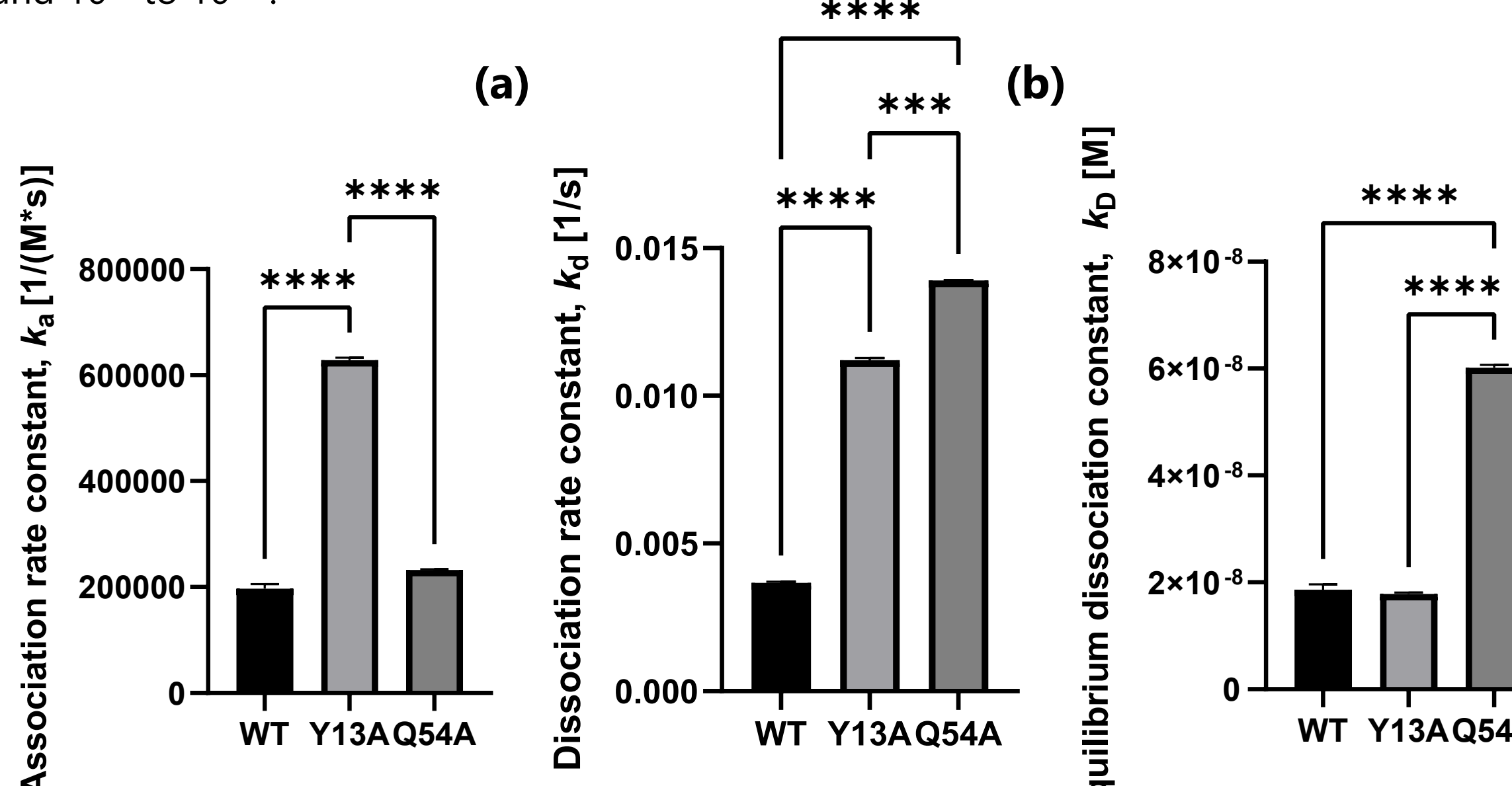


Figure 6: WT to mutant's kinetic constant comparison. (a) Dissociation rate constant graph. (b) Association rate constant graph. (c) Equilibrium dissociation constant (or affinity) graph. Analysis was done by one-way Brown-Forsythe and Welch ANOVA tests on GraphPad Prism 9. No asterisks denote a p-value > 0.05, [\*\*] denotes a p-value = 0.0001, and [\*\*\*\*] denotes a p-value < 0.0001. These are based on four differing concentrations for WT and Y13A as well as five concentrations for Q54A.

## Summary

- This data suggests that the Q54A mutation was statistically more unstable compared to the WT as indicated by a p-value < 0.0001 for  $k_D$  (i.e., affinity).
- The Y13A mutation is not statistically significant compared to the WT U1A indicated by a p-value < 0.05 for  $k_D$  (i.e., affinity).
- Potential Impact:** By studying U1A protein mutations, we may better our understanding of spliceosomal diseases and how much these mutations can affect the splicing of RNA within eukaryotic cells.
- Future works:** This study utilized an NTA biosensor to couple U1A via its His-tag. Another option is to chemically modify Biotin to U1A then use a Biotin biosensor instead - this is the approach primarily seen in the literature. In order to optimize our SPR protocol and better understand U1A-RNA kinetics, a comparison between NTA and Biotin biosensors could be beneficial.

## Acknowledgment

This study was supported by the PILOT program operating within the Burnett School of Biomedical Sciences, College of Medicine at the University of Central Florida. Dr. Kersten Schroeder allowed our use of the SPR instrument and provided training as well as mentoring. We would like to thank Dr. Hajeung Park for providing supplies and mentorship on protein mutation and purification. This study would not have been possible without Dr. Park.